EARTH'S CRYOSPHERE
SCIENTIFIC JOURNAL

Earth`s Cryosphere, 2018, vol. XXII, No. 5, pp. 17–25 **http://earthcryosphere.ru/**

THERMOPHYSICAL PROCESSES IN CRYOSPHERE

DOI: 10.21782/EC2541-9994-2018-5(17-25)

PHYSICAL MODELING OF SURFACE TEMPERATURE CONTRASTS ON SAMPLES OF TUNDRA SOIL COVER

S.G. Kornienko

Oil and Gas Research Institute, RAS, 3, Gubkina str., Moscow, 119333, Russia; spaceakm2@ogri.ru

The results of modeling temperature contrasts on the surface of single-layer and multi-layer columns containing samples of ground, substrate and tundra soil cover using an open-type simulation setup are provided, in which the temperature differences of varying permafrost conditions are simulated. Quantitative indicators of the extent of attenuation of temperature variations in the ground by lichen cover of different thickness are evaluated. Maximum (daytime) and minimum (night) values of the temperature on the surface of the samples do not differ significantly from the average values, indicating the possibility of investigating the nature of temperature anomalies on the surface of the tundra soil cover related to permafrost heterogeneity by simultaneous measurements of the soil surface temperature at any time of the day. The possibility of using the setup to characterize the thermophysical properties of soil samples and of the soil cover, as well as to study and simulate phase transitions of water, is demonstrated.

Permafrost heterogeneity, ground, temperature variations, soil cover, tundra, physical modeling

INTRODUCTION

Over the recent years, infrared remote sensing (IRS) has become broadly applicable to description of permafrost [*Leschack et al., 1973; Morrissey et al., 1986; Hachem et al., 2009; Langer et al., 2010*; *Muster et al., 2015; Ran et al., 2015; Westermann et al., 2015*]. Development of methods and accumulation of experience in this area are based on the theoretical possibility of mapping models of the state and behavior of permafrost landscapes, as well as of studying permafrost heterogeneities based on the ground temperatures, calculated on the basis of IRS data. In this case, permafrost heterogeneities are understood as any differences in the characteristics and parameters below the active layer, including temperature differences in the depths of zero amplitudes for fluctuations in ground temperatures, ice content, thermophysical characteristics of frozen soils, and the presence of cryopegs, which in total may influence the distribution of the ground surface temperature.

In most cases, the temperature of the ground and soil surface is interpreted as the temperature of the ground and soil at insignificant depths of 2–10 cm of the open ground or under the vegetation and soil cover (SC), to which mosses, lichens, low turf-fruticose and grassy species, turf and peat are referred. The temperature of the ground cover and soil is believed to be quite an informative parameter for describing and simulating permafrost [*Nelson et al., 1985; Heggem et al., 2006; Throop et al., 2012; Bobrik et al., 2015*], as opposed to the SC temperature. This is related to the fact that the surface itself is in the area of the most intense periodic and sporadic heat exchange processes, which include advective heat transfer in the ground air layer and evapotranspiration. Yet, it has been demonstrated in [*Hachem et al., 2009; Ran et al., 2015; Westermann et al., 2015*] that it is possible to make small-scale maps of the mean annual permafrost temperature and of the borderlines of permafrost distribution according to reanalysis data and to the mean annual values of the ground surface temperatures calculated on the basis of IRS data.

Another approach is based on evaluating the differences (contrasts) in the temperature of the ground surface areas with equal thermal inertia of the layer of daily temperature variations (DTV) in the period of the summer thaw [*Kornienko, 2012*]. The impact of advective heat transfer may be considered in repeated sensing sessions, while such interrelated parameters as evapotranspiration intensity, thermal inertia and the moisture content of the SC, substrate and ground may be determined on the basis of albedo, spectral indices and IRS data [*Sandholt et al., 2002; García et al., 2013; Girolimetto and Venturini, 2013; Minacapilli et al., 2016*]. At the same time, an essential issue is still to be resolved regarding the possibility of using the temperature of the tundra SC, as well as the temperatures of the ground (soil) surface, to characterize geocryological heterogeneities.

In general, not enough experiments have been conducted in this area, and the formation processes of the thermal regime and of the temperature on the surface of the tundra SC, including different geocryo-

Copyright © 2018 S.G. Kornienko, All rights reserved.

logical conditions, have been insufficientlly studied yet. The goal of this study was to simulate the temperature contrasts on the surface of the tundra SC and of the ground, using the experimental setup, imitating the temperature manifestations of geocryological heterogeneities.

THE METHODOLOGY OF THE STUDY AND THE CHARACTERISTIC OF THE SOIL COVER SAMPLES

Variations of the temperature field of the Earth's surface have daily and annual periodicity, and, in the absence of snow cover, the processes of crystallization of the soil moisture may be approximately described by the expression [*Pavlov, 1975*]:

$$T_s(\tau) = T_0 + \sum_{i=1}^{N} a_i \cos\left(\frac{2\pi}{t_i}\tau - \varphi_i\right), \qquad (1)$$

where T_0 – the mean annual temperature of the soil surface; a_i – the amplitude of the temperature variations of an individual harmonica on the ground surface; t_i – the variation period; τ – time; φ_i – the initial phase of the variations; N – the number of harmonicas; i – the harmonica number. The value of T_0 depends on the permafrost temperature at the depth of zero amplitudes for fluctuations in ground temperatures, whereas the amplitudes of DTV and the annual temperature variations (ATV) of the soil surface depend on the thermophysical characteristics of the respective DTV and ATV layers. For the tundra regions, the thickness of the DTV layer varies from 0.4 to 1.0 m, and the thickness of the ATV layer is 10–15 m.

It follows from equation (1) that theoretically the conditions of insolation, wind velocity, air temperature and moisture being equal, in the areas with equal thermophysical characteristics of the DTV layer, the difference of the temperatures on their surface $T_s(\tau)$ may carry information on the differences of the permafrost temperature and thermophysical characteristics of the ATV layer, related to geocryological heterogeneities. The contribution of the latter to the resulting temperature field on the surface does not exceed several degrees [*Leschack et al., 1973; Kornienko and Razumov, 2009*]. In the physical model, there is a possibility of "turning on" and "off" the temperature manifestations, simulating the impact of geocryological heterogeneities, which allows their contribution against other factors to formation of the thermal regime of SC.

The goal was to model similar temperature manifestations (temperature contrasts) on single-layer and multi-layer columns, which included samples of the tundra SC, substrate and soil. In this case, the temperature contrast implies the temperature difference between two columns on their lower border (ΔT_{lb}), on the surface (ΔT_s) and in air (ΔT_a) above the surface. The configuration of the setup is close in its design to the known devices for determining thermophysical characteristics of the samples of soil, ground and snow by the method of stable thermal impact [*Ershov, 2004; Riche and Schneebeli, 2013; Brovka et al., 2016*]. A distinctive feature of the proposed setup consists in the use of two equal containers open on top (Fig. 1) with columns, which allows temperature contrasts to be determined under natural conditions of daily and meteorological variations of the air moisture and temperature.

The dimensions of the internal part of each container were 25 × 25 × 32 cm, the containers' bottom

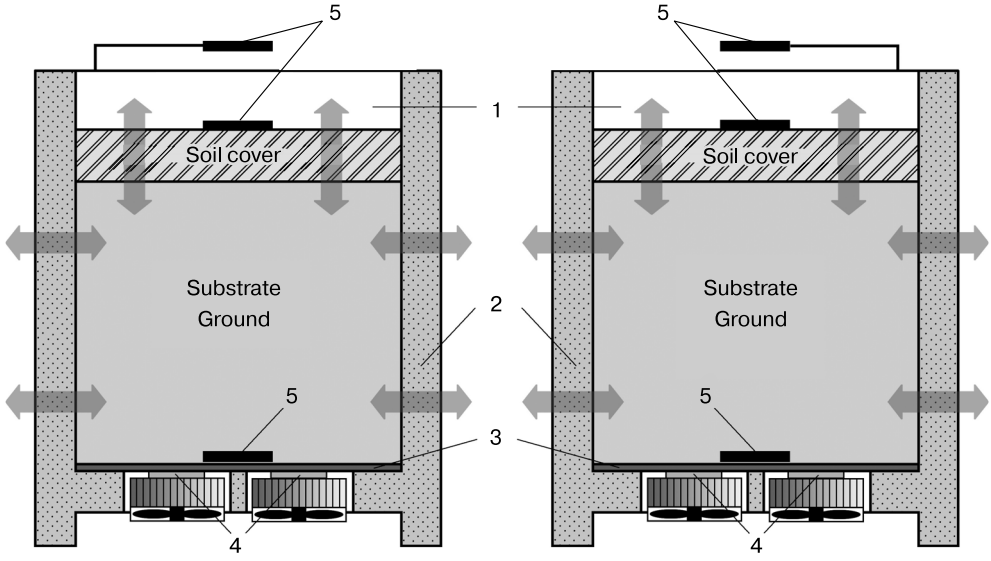

Fig. 1. The setup for simulating temperature contrasts on the surface of the samples of the tundra soil cover.

1 – the outer walls of the containers; 2 – heat insulation of the container walls; 3 – dural sheets; 4 – Peltier elements with radiators and cooling fans; 5 – temperature gauges (loggers).

was made of a dural plate 2 mm thick, the containers' walls and bottom insulated by polyurethane foam 3 cm thick. On the external side of the dural plate, two semiconductor Peltier elements were mounted, ensuring decrease or increase of temperature in the lower part of the container to 16 °C versus the temperature of the environment. To ensure equal conditions of heat exchange between the container walls and the environment, the containers were mounted on legs 25 cm above the floor. The temperature gauges (loggers) were mounted near the containers' bottom, on the columns' surface and higher, at the distance of 5 cm from the surface to control the ambient air temperature. In the sample, coupled temperature loggers HOBO U23-003 (OnSet, USA) were used with measurement precision of 0.2 °C. The loggers were mounted on the central vertical axis of the containers.

In the experiment, one of the containers gets alternately cooled or heated, resulting in the temperature contrast between the columns, including their surface. Cooling (heating) of the columns was maintained constant for several days creating an additional constant component complementary to the seasonal, daily, and meteorological temperature variations. As the container walls' isolation is not ideal, to ensure temperature contrasts on the columns' surface $\Delta T_s = 1–2$ °C, the temperature contrasts ΔT_{lb} were set within the range of 9–16 °C.

Table 1 contains characteristics of the samples of the tundra SC, substrate and ground, constituting five columns under study, alternately placed into the containers. The cover samples with their own substrate were taken in the area of the Yamburg oil and gas condensate field.

Table 1. **Characteristics of the samples of the soil cover, substrate and ground in the columns**

Column	Composition of samples in the column	Thickness, cm
C1	Moss *Polytrichum commune* with inclusions of grass	20
	Loamy substrate	5
C2	Lichen *Cladonia arbuscula*	7
	Garden (peat) ground	18
C3	Garden (peat) ground	25
C4	Moss *Polytrichum commune*	11
	Garden (peat) ground	20
C5	Moss *Polytrichum commune*	12
	Garden (peat) ground	18

Shown in Fig. 2 are the photographs of columns C1 and C2 with the container sides removed, the cover thickness values are indicated. Column C1 is composed of a rather thick layer of moss with its own clay loam substrate. In the sample of lichen SC in column C2, the thickness of its own clay loam substrate did not exceed 1 cm. Column C3 is represented by homogeneous garden peat. In the identical moss samples in columns C4 and C5, the thickness of its own clay loam substrate did not exceed 1 cm, either.

The setup was placed outdoors in the shade in open air; all the measurements were made in Moscow

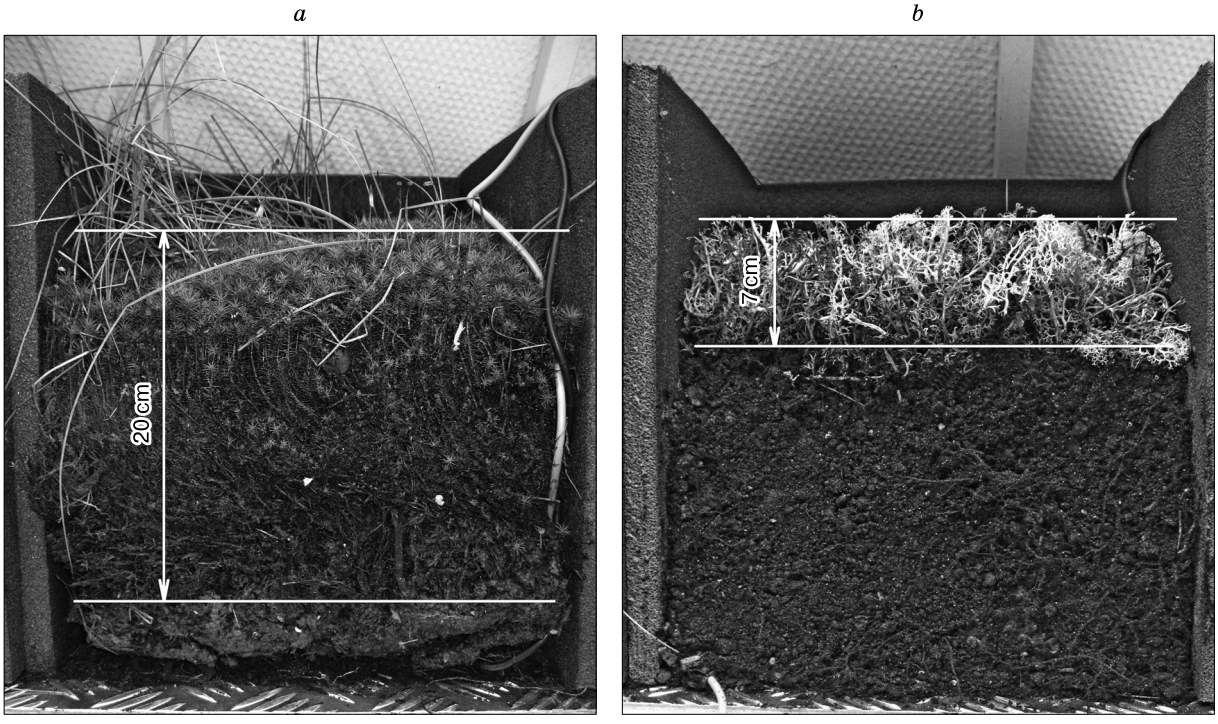

Fig. 2. The side view of the containers having columns C1 (*a*) and C2 (*b*) with samples of soil cover.

in the summer-autumn periods of 2013–2014 before the onset of the autumn frosts. During the measurements, the maximum air temperature reached 35 °C, and the minimum temperature was 5 °C. During the experiment, the volumetric content of water in the columns was maintained at the level of 12–14 %; loggers EC-5 (Decagon Devices Inc., USA) were used to control the water content. The experiment consisted of three cycles of measurements, each of which included the periods of alternate cooling (heating) of the columns, as well as of the background periods without cooling (heating). Duration of the cycles was 27, 13 and 43 days; duration of the periods of cooling (heating) of the columns with the samples varied from 4 to 14 days. The temperature values were recorded during a day with a 5 min. interval. Analysis and processing of the data were conducted with the HOBO Pro BHW software program, supplied together with the loggers, and with the Excel program of the standard Microsoft Office package.

The background (additive) components of the temperature contrasts, related to differences in the thermophysical characteristics of the columns, as well as to the impact of other factors, like the differences in the containers' insulation, air circulation details, etc., were measured by the measurements made in-between the periods of cooling (heating). Based on these data, corrections were made for each cycle, which allowed the differences between the background components of the values of ΔT_{lb}, ΔT_s and ΔT_a to be determined. In data processing, the days of switching off cooling (heating) were excluded, as well as the days of significant (>10 °C) rises in the daily air temperature.

The relation between the contrasts ΔT_{lb}, ΔT_s and ΔT_a was primarily evaluated by the mean daily values of the temperature, which decreased the impact of random factors. In a similar way, relations between these parameters by maximum (day) and minimum (night) temperature values were estimated. For this purpose, the temperature values for each hour were averaged, and maximum and minimum (for a day) values were chosen. As the intensity of cooling (heating) in cycles was not always the same, to compare the influence of the SC types on temperature contrasts ΔT_s, the gain factor $G = \Delta T_s/\Delta T_{lb}$ was used. The values of the temperature contrasts were always determined as the difference in the temperatures between (arbitrarily) the first and the second container.

THE RESULTS OF MODELING THE TEMPERATURE CONTRASTS ON THE SURFACE OF SOIL SAMPLES AND OF THE SOIL COVER

Shown in Fig. 3 are two days' thermogram columns C2 in the background period and in the period of cooling on the lower boundary. The measurements are shown averaged by 1 hour and refer to the second cycles of the observations, which were conducted in October 2013. It can be seen from comparison of the thermograms that when the sample was cooled, the surface temperature of the C sample significantly decreased versus the air temperature.

Figure 4 contains curves characterizing the change in the mean daily temperature contrasts in the first cycles of the observations at cooling of column C3 (ground, Zone *A*) and column C1 (moss, Zone *B*). Column C3 was placed in the second container; therefore, the temperature contrasts at the lower boundary and on the surface of column C3 are shown with a positive sign. Hereinafter, the measurement results are provided with corrections for the difference with the background components of the temperature contrasts. It can be seen from Fig. 4 that contrast ΔT_s depends on ΔT_{lb} and is not related to ΔT_a, the values of which are close to zero. For column C3 containing homogeneous ground at lower values of ΔT_{lb} (Zone *A*), higher values of ΔT_s are recorded, compared to column C1 (Zone *B*), consisting mainly of moss.

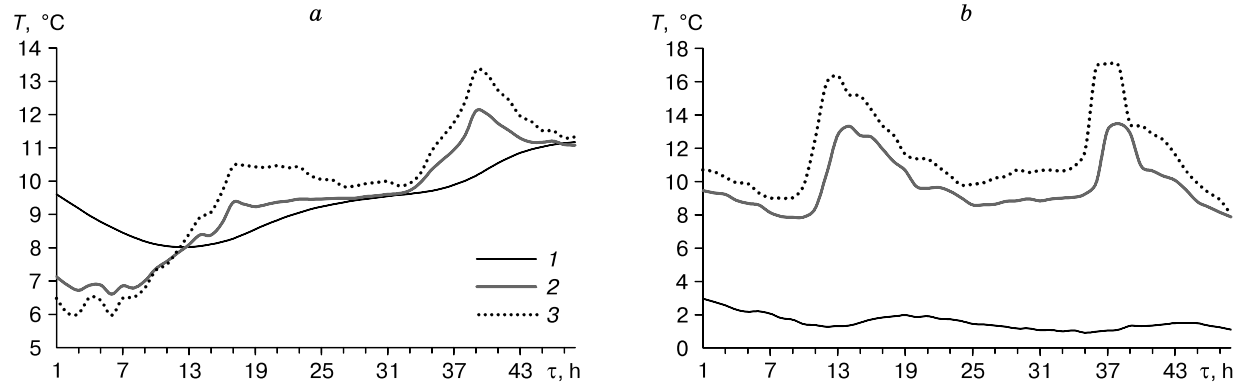

Fig. 3. Thermograms of column C2 in the background period (*a*) and in the period of artificial cooling from below (*b*).

1 – the temperature at the lower boundary; *2* – the temperature on the surface of the SC sample; *3* – the air temperature above the SC sample.

For the same pair of columns, statistical relations were considered between the mean daily values of ΔT_s and ΔT_{lb} (Fig. 5, *a*) and between ΔT_a and ΔT_s (Fig. 5, *b*). Here the relation between ΔT_s and ΔT_{lb} is confirmed by the rather high value of the correlation index ($R = 0.957$), while the difference in the intensity of temperature contrasts on the surface of the ground (*A*) and moss (*B*) is attributed to different slopes of the areas of the approximating function (Fig. 5, *a*). Relatively low correlation ($R = 0.658$) between ΔT_a and ΔT_s (Fig. 5, *b*) and the variance of the values of ΔT_a, lower by an order of magnitude compared to ΔT_s indicates the absence of the impact of the air temperature on the soil surface and the possible influence of the soil surface temperature (cooled from below) on the temperature of air near the soil surface.

In the second measurement cycle, column C1 remained in the first container, while column C3 was

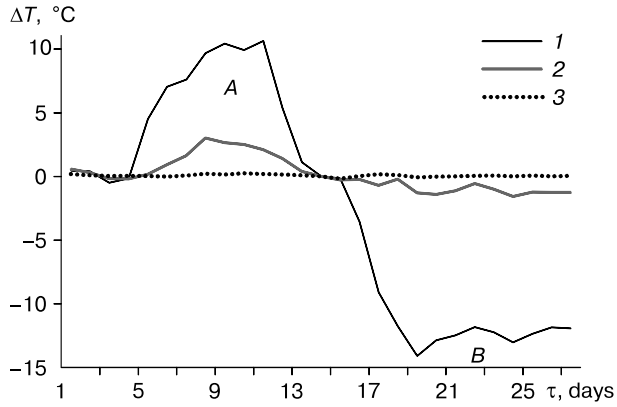

Fig. 4. Changes in the mean daily values of the temperature contrasts at cooling of columns C3 (*A*) and C1 (*B*) in the first measurement cycle.

1 – ΔT_{lb}; *2* – ΔT_s; *3* – ΔT_a.

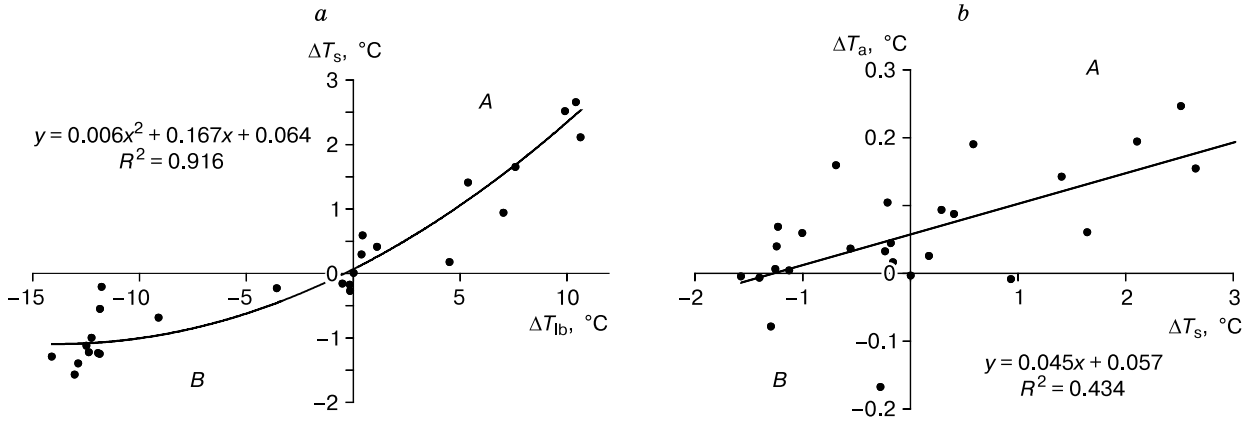

Fig. 5. The relation of the mean daily values ΔT_s and ΔT_{lb} (*a*), ΔT_a and ΔT_s (*b*) at cooling of columns C3 (*A*) and C1 (*B*).

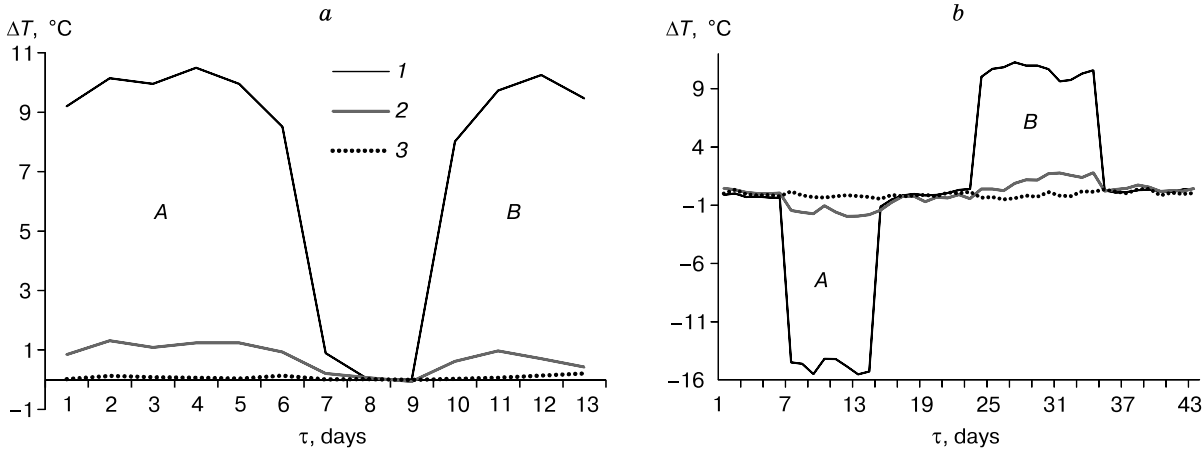

Fig. 6. Changes in the mean daily values of the temperature contrasts at heating of column C1 (*A*) and cooling of column C2 (*B*) in the second measurement cycle (*a*) and at cooling of columns C4 (*A*) and C5 (*B*) in the third measurement cycle (*b*).

1 – ΔT_{lb}; *2* – ΔT_s; *3* – ΔT_a.

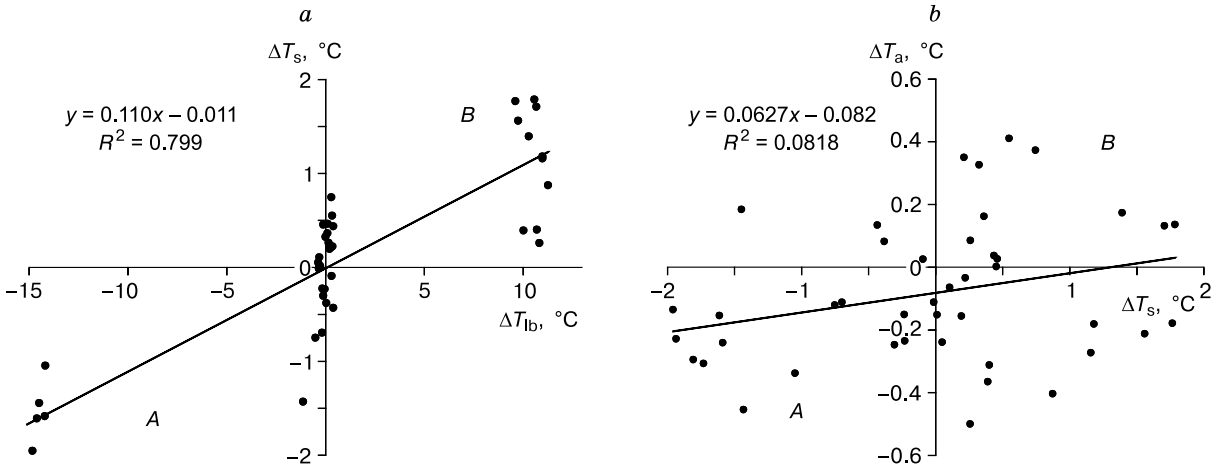

Fig. 7. The relation of the mean daily values ΔT_s and ΔT_{lb} (*a*), ΔT_a and ΔT_s (*b*) at cooling of columns C4 (*A*) and C5 (*B*).

replaced by column C2 containing the same ground and lichen SC. The configuration of the second-cycle is shown in Fig. 2. First column C1 (Zone *A*) was heated, and then, after the background period, column C2 (Zone *B*, Fig. 6, *a*) was cooled. Here, too, like in the previous case, it is clear that ΔT_s depends on ΔT_{lb}. The rather high correlation index between ΔT_s and ΔT_{lb} ($R = 0.867$) is significant at $p < 0.05$, whereas for parameters ΔT_a and ΔT_s its relatively low value ($R = 0.302$) is not significant for the same value of p.

In the third, longest, measurement cycle of columns C4 (Zone *A*) and C5 (Zone *B*, Fig. 6, *b*) with identical composition of the soil and SC were cooled. The measurement results are generally similar to those in the first two cycles. Statistical relations between the mean daily values of ΔT_s and ΔT_{lb}, ΔT_a and ΔT_s for this pair of columns are shown in Fig. 7. The correlation index $R = 0.894$ between ΔT_s and ΔT_{lb} (Fig. 7, *a*) is significant at $p < 0.05$. The values ΔT_s and ΔT_{lb} are grouped into three clusters corresponding to the period of cooling of columns C4 (*A*) and C5 (*B*), as well as to the background period with the values of ΔT_{lb} close to zero. The relation between ΔT_a and ΔT_s ($R = 0.286$) is practically absent here (Fig. 7, *b*).

Table 2 shows the values of contrasts of the mean daily, maximum and minimum daily temperatures averaged for the periods of cooling (heating) on the lower boundary and on the surface of the columns, as well as the respective values of the gain factor *G*.

Table 2. **The values of temperature contrasts of the mean daily, maximum and minimum temperatures and of the gain factor (*G*) at cooling and heating of the columns**

Cycle	Column	ΔT_{lb}, °C	ΔT_s, °C	$G = \Delta T_s/\Delta T_{lb}$
1	C1 (cooling, mean daily)	–11.42	– 0.98	0.086
	C1 (cooling, max)	–12.99	–1.08	0.083
	C1 (cooling, min)	–12.55	–1.16	0.092
	C3 (cooling, mean daily)	9.22	2.14	0.232
	C3 (cooling, max)	9.27	2.08	0.224
	C3 (cooling, min)	8.65	1.81	0.209
2	C1 (heating, mean daily)	9.71	1.10	0.113
	C1 (heating, max)	10.44	1.27	0.121
	C1 (heating, min)	9.18	0.98	0.107
	C2 (cooling, mean daily)	9.80	0.97	0.099
	C2 (cooling, max)	9.52	0.98	0.103
	C2 (cooling, min)	9.20	0.99	0.107
3	C4 (cooling, mean daily)	–15.77	–1.66	0.105
	C4 (cooling, max)	–15.44	–1.39	0.090
	C4 (cooling, min)	–16.19	–1.51	0.093
	C5 (cooling, mean daily)	10.88	1.27	0.116
	C5 (cooling, max)	10.33	1.33	0.128
	C 5 (cooling, min)	11.60	1.63	0.140

DISCUSSION OF RESULTS

The results obtained indicate the possibility of using the setup with two alternately cooled (heated) containers with samples of ground and of tundra SC to ensure evaluation of the relation between the temperature on the surface of the columns and the temperature on their lower boundary. Rather high correlation of the values of ΔT_s and ΔT_{lb} and relatively low correlation of ΔT_a and ΔT_s for all the observation cycles clearly testify to the dependence of ΔT_s on ΔT_{lb}. It follows from Table 2 that the gain factors *G*, which in fact characterize the thermophysical properties of the columns, may differ by a factor of 2 or 3. The highest values of *G* refer to column C3 containing garden ground without SC, which could be expected, considering its higher thermal conductivity coefficient, compared to the SC samples. In column C2 having the same ground but lichen cover, the gain factor *G* is approximately 2 times less than in column C3.

For columns C1, C4 и C5 having samples of the moss cover, the values of G differ not so significantly. At heating of column C1, the value of G is approximately 30 % higher than at its heating, which may be related to the increase in the share of the convective component of heat exchange in the thick layer of moss at heating from below. At the same time, the gain factor G of column C1 (at cooling) is somewhat lower, which may be related to lower thickness of the moss samples in C4 and C5.

As the experimental conditions simulate the process of stationary heat transfer, it is possible, based on simple equations, approximately to calculate the temperature contrasts at any distance from the bottom to the surface of column C3 with ground, as well as in column C2 under the lichen SC with the same ground, considering the same height of the columns and admitting that the thermal conductivity coefficients of the ground in the columns are equal. In the background periods, the air temperature around the containers is approximately the same; therefore, the mean daily values of the temperature at the lower boundary and on the surface of the columns differ insignificantly. Therefore, we may admit that the mean daily values of the heat fluxes and temperature gradients in the columns are equal to zero in the background periods. Then we can assume that in the periods of cooling (heating) the temperature gradients in the columns would depend only on the value of the temperature contrast achieved at the lower boundary. The temperature gradient in column C3 with ground ($T_{g,\,C3}$) is determined by the formula

$$\mathrm{grad}\left(T_{g,C3}\right)=\frac{\Delta T_{lb,C3}-\Delta T_{s,C3}}{L}, \qquad (2)$$

where $\Delta T_{lb,\,C3}$, $\Delta T_{s,\,C3}$ – mean daily values of the temperature contrasts at the lower boundary and on the surface of the open ground of column C3, respectively (Table 2); L – length (height) of columns C3 and C2 (Table 1). As in this case the temperature gradient depends only on the temperature contrasts at the lower boundary, the temperature gradient in the ground in column C2 ($T_{g,\,C2}$) may be determined by the formula

$$\mathrm{grad}\left(T_{g,C2}\right)=\mathrm{grad}\left(T_{g,C3}\right)\frac{\Delta T_{lb,C2}}{\Delta T_{lb,C3}},$$

where $\Delta T_{lb,\,C2}$ – the mean daily value of the temperature contrast at the lower boundary of column C2 (Table 2). The temperature contrast in column C2 on the boundary between the ground and SC ($\Delta T_{gsc,\,C2}$) is determined by the formula

$$\Delta T_{gsc,\,C2}=\Delta T_{lb,C2}-\mathrm{grad}\,(\Delta T_{g,C2})\cdot(L-d), \qquad (3)$$

where d – SC thickness in column C2 (Table 1). In this case, the calculated value of the temperature contrast at the boundary between the soil and SC in column C2 (with d = 7 cm) was 4.38 °C. The value of the temperature gradient in SC of column C2 was calculated in a similar way (2) by the values $\Delta T_{gsc,\,C2}$ and $\Delta T_{s,\,C2}$ (Table 2):

$$\mathrm{grad}\left(T_{sc,C2}\right)=\frac{\Delta T_{gsc,C2}-\Delta T_{s,C2}}{d}.$$

The relation of the temperature gradients in SC and in the ground of column C2 demonstrates that the thermal conductivity coefficient of the ground is 1.61 times higher than that of SC. The temperature contrasts of the SC surface of column C2 for d = 0–7 cm were calculated by the formula

$$\Delta T_{s,C2}(d)=$$
$$=\left[\Delta T_{lb,C2}-\mathrm{grad}\left(T_{g,C2}\right)\cdot(L-d)\right]-\mathrm{grad}\left(T_{sc,C2}\right)\cdot d.$$

The degree of attenuation of the temperature contrast by the SC layer in column C2 may be expressed as coefficient $E = \Delta T_{gsc,\,C2}/\Delta T_{s,\,C2}(d)$. Dependence of coefficient E on d is provided in Fig. 8.

In accordance with (3), with d = 0 (i.e., hypothetically, when column C2 wholly consists of ground), the temperature contrast on the surface of $\Delta T_{lb,\,C2}$ = 2.28 °C. Given the same temperature contrast on the lower boundary and the same column height, the measured mean value of the temperature contrast on the surface of the lichen SC ($\Delta T_{s,\,C2}$) was 0.97 °C (Table 2). The relation between these parameters may be expressed by coefficient $P = \Delta T_{lb,\,C2}/\Delta T_{s,\,C2}(d)$. Given the constant value of $\Delta T_{lb,\,C2}$ = = 2.28 °C, dependence of coefficient P on d is also shown in Fig. 8. Coefficient P shows by how many factors, depending on the SC thickness, the temperature contrasts on its surface may differ from those on the surface of open ground, with the temperature contrasts at the lower boundary equal for the column height.

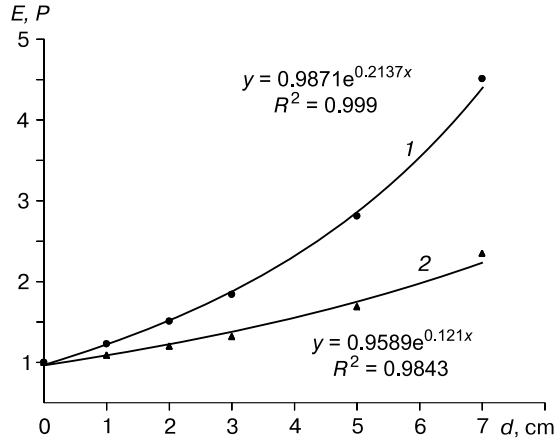

Fig. 8. Dependence of coefficients E (curve *1*) and P (curve *2*) of attenuation of the temperature contrasts on thickness d of the lichen soil cover.

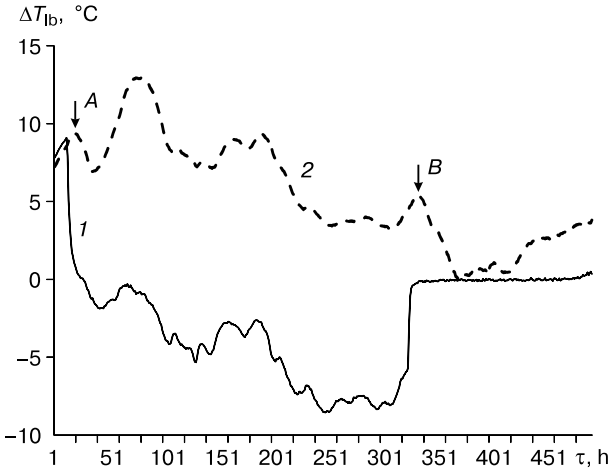

Fig. 9. The temperature behavior at the lower boundary (T_{lb}) of columns C1 (curve *1*) and C3 (curve *2*) with a phase transition period in column C1.

For each column, the mean daily, maximum and minimum values of coefficient *G* differ insignificantly (Table 2) and do not violate the general relation between the temperature contrasts and the column types. All the above is true of the results of simultaneous measurements at any time of the day.

If slightly upgraded, the setup described may be used for determining the effective values of thermal conductivity coefficients of single-layer and multilayer columns with samples of solid and loose ground, substrate and tundra SC in any combination of the components, including their dependence on their own water content and air moisture. The setup may be also used for studying and simulating phase transitions in grounds and substrates, with their differing water content and salinity. Fig. 9 provides curves demonstrating the temperature behavior (1 hour averaging) at the lower boundary of the cooled column C1 and column C3. The arrows indicate moments of switching on (*A*) and off (*B*) of cooling. At the beginning of freezing (moment *A*), no signs of phase transition were recorded at transition of the temperature at 0 °C, which is related to the relatively low water content of the ground in the period of cooling. After switching off cooling and watering of both columns (moment *B*), the condition of five days' phase transition was registered for column C1.

In general, the results obtained may be useful in studying the nature of temperature anomalies on the surface of the tundra soil cover related to geocryological heterogeneities.

CONCLUSIONS

An open-type setup has been developed and tested having two cooled (heated) containers containing samples of ground, substrate and tundra soil cover, which allows simulation of temperature contrasts on their surface related to geocryological heterogeneities.

Based on the values of temperature contrasts at the boundary between the ground and the lichen soil cover, on the surface of open ground and the surface of the soil cover, the dependences have been determined, characterizing the degrees of attenuation of the temperature contrasts in the ground by the soil cover of different degrees of thickness.

Maximum (day) and minimum (night) values of the temperature contrasts on the samples' surface do not significantly differ from the mean daily values, indicating the possibility of studying the nature of temperature anomalies on the surface of the tundra soil cover, including those related to geocryological heterogeneities, by simultaneous measurements of temperature contrasts of the soil cover surface at different time of the day.

The setup may be used for determining effective values of thermal conductivity coefficients of one- and many-layer columns with samples of solid and loose ground, substrate and tundra soil cover, as well as for modeling phase transitions in grounds and substrates.

References

Bobrik, A.A., Goncharova, O.Yu., Matyshak, G.V., et al., 2015. Correlation of active layer thickness and landscape parameters of peatlands in the northern of West Siberia (Nadym station). Earth's Cryosphere (Kriosfera Zemli) XIX (4), 29–35.

Brovka, G.P., Agutin, K.A., Brovka, A.G., et al., 2016. A complex of methods of experimental study of the processes of heat and mass conduction and soil bulging in freezing soils and alpine rocks, in: Proceedings of the Fifth Conference of Permafrost Scientists of Russia, June 14–17, 2016). Universitetskaya Kniga, Moscow, pp. 11–17.

Ershov, E.D. (Ed.), 2004. Methods of Geocryological Studies: a textbook. Moscow University Press, Moscow, 512 pp. (in Russian)

García, M., Sandholt, I., Ceccato, P., et al., 2013. Actual evapotranspiration in drylands derived from in-situ and satellite data: Assessing biophysical constraints. Remote Sens. Environ., 131, 103–118.

Girolimetto, D., Venturini, V., 2013. Water stress estimation from NDVI-Ts plot and the wet environment evapotranspiration. Adv. Remote Sens., No. 2, 283–291.

Hachem, S., Allard, M., Duguay, C., 2009. Using the MODIS land surface temperature product for mapping permafrost: an application to northern Quebec and Labrador, Canada. Permafrost and Periglacial Processes 20, 407–416.

Heggem, E.S.F., Etzelmüller, B., Anarmaa, S., et al., 2006. Spatial distribution of ground surface temperatures and active layer depths in the Hövsgöl area, northern Mongolia. Permafrost and Periglacial Processes 17 (4), 357–369.

Kornienko, S.G., 2012. The method of evaluating the ice content of frozen soil based on remote sensing data in the visible and infrared bands. Issledovanie Zemli is Kosmosa, No. 5, 75–84.

Kornienko, S.G., Razumov, S.O., 2009. Modelling of temperature contrasts on the surface of inhomogeneous ice content in the ground. Kriosfera Zemli XIII (2), 55–61.

Langer, M., Westermann, S., Boike, J., 2010. Spatial and temporal variations of summer surface temperatures of wet polygonal tundra in Siberia – implications for MODIS LST based permafrost monitoring. Remote Sens. Environ. 114, 2059–2069.

Leschack, L., Morse, F., Brinley, W., et al., 1973. Potential use of airborne dual-channel infrared scanning to detect massive ice in permafrost, in: North American Contribution Permafrost. Second International Conference, USA, Washington, D.C., pp. 542–549.

Minacapilli, M., Consoli, S., Vanella, D., et al., 2016. A time domain triangle method approach to estimate actual evapotranspiration: Application in a Mediterranean region using MODIS and MSG-SEVIRI products. Remote Sens. Environ. 174, 10–23.

Morrissey, L., Strong, L., Card, D., 1986. Mapping permafrost in the boreal forest with Thematic Mapper satellite data. Photogramm. Eng. Remote Sens. 52 (9), 1513–1520.

Muster, S., Langer, M., Abnizova, A., et al., 2015. Spatio-temporal sensitivity of MODIS land surface temperature anomalies indicates high potential for large-scale land cover change detection in Arctic permafrost landscapes. Remote Sens. Environ. 168, 1–12.

Nelson, F., Outcalt, S., Goodwin, C., et al., 1985. Diurnal thermal regime in a peat-covered palsa, Toolik lake, Alaska. Arctic 38 (4), 310–315.

Pavlov, A.V., 1975. Heat Exchange between Soil and Atmosphere in Northern and Temperate Latitudes of the USSR Territory. Yakutsk Publishing House, Yakutsk, 304 pp. (in Russian)

Ran, Y., Li, X., Jin, R., et al., 2015. Remote sensing of the mean annual surface temperature and surface frost number for mapping permafrost in China. Arctic, Antarctic, and Alpine Research 47 (2), 255–265.

Riche, F., Schneebeli, M., 2013. Thermal conductivity of snow measured by three independent methods and anisotropy considerations. The Cryosphere 7, 217–227.

Sandholt, I., Rasmussen, K., Andersen, J., 2002. A simple interpretation of the surface temperature/vegetation index space for assessment of surface moisture status. Remote Sens. Environ. 79, 213–224.

Throop, J., Lewkowicz, A., Smith, S., 2012. Climate and ground temperature relations at sites across the continuous and discontinuous permafrost zones, northern Canada. Canadian J. Earth Sciences 49 (8), 865–876.

Westermann, S., Ostby, T., Gisnas, K., et al., 2015. A ground temperature map of the North Atlantic permafrost region based on remote sensing and reanalysis data. The Cryosphere 9, 1303–1319.

Received July 12, 2017